Effect of Shear Stud Layout on the Seismic Behavior of Slab-Column Connections

E. Matzke & C.K. Shield
University of Minnesota

G.J. Parra-Montesinos
University of Michigan

M.-Y. Cheng
National Taiwan University of Science & Technology

SUMMARY:
Results from large-scale tests of slab-column connections with various shear stud arrangements are presented. Each test specimen consisted of nearly a full-scale, first-story interior slab-column connection and was subjected to combined gravity load and bi-axial lateral displacement reversals. The amount of gravity load was selected such as to induce a gravity shear ratio of ½. The main experimental test variables were: 1) shear stud spacing within each peripheral line, and 2) ratio between ACI Code-calculated shear strength provided by shear studs and expected shear demand.

All test specimens ultimately failed by punching, but drift capacity varied between 0.90% and 2.30% in each direction (1.25% and 3.25% resultant drift) depending on the amount and distribution of shear studs. Best behavior was exhibited by a specimen in which shear studs were designed to resist the entire shear demand due to gravity load and unbalanced moment, with spacing limited to 0.5*d* between adjacent stud peripheral lines and to 1.5*d* between studs within the first three peripheral lines.

Keywords: punching shear, drift capacity, two-way slabs, shear reinforcement, bi-axial displacements

1. INTRODUCTION

Slab-column frame systems are often used in earthquake-prone regions in combination with structural walls or beam-column frames. Although typically not designed to resist earthquake-induced forces, slab-column frames must be capable of maintaining their gravity load carrying capacity under earthquake-induced displacements. In order to ensure adequate punching shear strength and deformation capacity of slab-column connections when subjected to ground motions, structural designers often rely on shear reinforcement. In the US, headed studs supported by steel plates (rails), oriented perpendicularly to the column faces forming a cruciform layout, are a common preference of structural designers and contractors.

In this paper, results from tests of nearly full-scale slab-column connections subjected to combined gravity load and bi-axial lateral displacements are presented. The main objective of the tests was to evaluate the influence of shear stud amount and layout on the behavior of slab-column connections and in particular, drift capacity.

2. ACI CODE DESIGN PROVISIONS FOR SHEAR STUD REINFORCEMENT

Design provisions for headed shear stud reinforcement were first introduced to the ACI Building Code in 2008 (ACI Committee 318, 2008). The nominal punching shear strength of slab-column connections, v_n, is taken equal to the summation of a "concrete" contribution, v_c, and a steel reinforcement contribution, v_s (Eq. 2.1). When shear studs are provided, the following stress limitations apply,

$$v_n = v_c + v_s \leq \frac{2}{3}\sqrt{f_c'} \text{ (MPa)} \tag{2.1}$$

$$v_s = \frac{A_v f_y}{s b_o} \geq \frac{1}{6}\sqrt{f_c'} \text{ (MPa)} \tag{2.2}$$

where A_v is the total cross-sectional area of the shear stud shanks in a single peripheral line of shear studs, f_y is the stud yield strength, s is the spacing between adjacent peripheral lines of shear studs, and b_o is the length of the critical shear perimeter. For interior square columns, v_c = (1/4) $\sqrt{f_c'}$ (MPa). It is worth mentioning that the allowable shear stress limit of (2/3) $\sqrt{f_c'}$ (MPa) and the so-called concrete contribution of (1/4) $\sqrt{f_c'}$ (MPa) are 4/3 and 3/2 times larger than what is allowed when other types of shear reinforcement are used. These increased stress values were based on recommendations by Dilger and Ghali (1981), who claimed that headed shear studs provide better anchorage than other types of shear reinforcement.

For slab-column connections that may be subjected to earthquake-induced displacements and designated not to be part of the seismic-force-resisting-system, in addition to gravity load design considerations, Chapter 21 of the 2008 ACI Building Code requires $v_s \geq 0.29\sqrt{f_c'}$ (MPa) over at least four times the slab thickness from the column faces, unless either 1) the shear stress demand due to gravity shear and unbalanced moment at the design lateral displacement does not exceed the design shear strength of the connection determined according to Chapter 11, or 2) the design drift does not exceed the larger of 0.005 and [$0.035-0.05v_{ug}/(\phi\, v_c)$], where v_{ug} is the shear stress due to gravity load and $\phi = 0.75$.

Spacing limits for shear stud reinforcement are provided in Chapter 11. In non-prestressed slabs, spacing between peripheral lines of shear studs is limited to either 0.5d or 0.75d depending on the shear stress demand. Also, a spacing limit of 2d is specified between studs in the first peripheral line. The lack of a spacing limit within each peripheral line other than that closest to the column allows the use of shear studs in a cruciform pattern, where rails of studs extend perpendicularly away from each column face. To date, this has been a common the preferred layout for structural designers and contractors in the US. It is worth mentioning that in the recently released recommendations by ACI Committee 352 (2011) the 2d peripheral spacing limit also applies to the second peripheral line. Further, the ACI Code spacing provisions contrast with those in the Eurocode (Comité Européen de Normalisation, 2004), where a maximum spacing limit of 1.5d is applied to several peripheral lines of studs, and a limit is also imposed to the width of the slab engaged by the shear studs. The result is thus a more uniform distribution of shear reinforcement around the column compared to that obtained following a cruciform pattern.

3. EXPERIMENTAL PROGRAM

A total of five nearly full-scale slab-column connections with shear stud reinforcement were tested under combined gravity load and bi-axial lateral displacements at the University of Minnesota NEES-MAST Laboratory. Due to space limitations, however, focus will be placed on three of the test specimens.

Each specimen represented a first-story interior connection subassembly. The column at the base of each subassembly was fixed to a concrete base block anchored to the laboratory strong floor. The slab was supported at each corner by a hydraulic actuator and stiffened along its perimeter by steel tube sections (Figure 3.1). The column extended approximately half a story above the slab, where lateral displacements were applied assuming an inflection point at this location. Figure 3.1 shows an elevation view of the test specimens.

3.1 Specimen Design

The slab in the test specimens was 5.2x5.2x0.15 m, supported by a 0.4 m square column. Because the slab-column connections were considered not to be part of the seismic-force-resisting system, only gravity loads were considered for design of the flexural reinforcement in the slab. The slab flexural reinforcement was designed to resist gravity loads with intensity such as to create an average shear stress equal to $(1/6)\sqrt{f_c'}$ (MPa) (gravity shear ratio of 0.5) on the critical section of the connection, defined by a distance of $d/2$ from each column face. For this purpose, a *DL* to *LL* ratio of 2 was assumed, where *DL* and *LL* are the dead load and live load intensities, respectively. While the load combination of 1.2*DL*+1.6*LL* governed the flexural design of the slab, the gravity shear stress was calculated based on 1.2*DL*+0.5*LL*, as specified in Chapter 21 of the 2008 ACI Code. Reinforcement was then selected based on these design loads using the Direct Design Method outlined in Section 13.6 of the ACI Code (ACI Committee 318, 2008). The reinforcement design resulted in a relatively low, but realistic, top reinforcement ratio of 0.6% in the column strip (based on the slab thickness). The top and bottom reinforcement layout is shown in Figure 3.2. The top reinforcement ratio of 0.6% is substantially lower than that typically used in slab-column connection tests with shear stud reinforcement (for example, Megally and Ghali, 2000), in which tensile reinforcement ratios as high as 1.5% are often used to force a punching shear failure with limited or no flexural yielding. Given the relationship between punching shear strength and flexural reinforcement ratio (Widianto et al., 2009), such approach may lead to unrealistically high punching shear strengths and does not allow a proper evaluation of the effect of flexural yielding on the punching shear capacity of slabs subjected to earthquake-induced displacements.

The slab in all three specimens described in this paper had the same flexural reinforcement layout. Different shear reinforcement designs were implemented, however, to evaluate their effectiveness to resist two-way shear stresses and increase ductility when subjected to earthquake-type loading. A simple notation is used to identify the three specimens, based on the layout and amount of shear stud reinforcement used. The first two letters refer to the overall layout, CR for cruciform and RA for radial-type layout. The number that follows refers to the value of the concrete contribution v_c used in design, as a function of $\sqrt{f_c'}$ (MPa). For example, Specimen CR-1/4 represents a specimen with a cruciform shear stud layout in which a concrete contribution $v_c = (1/4)\sqrt{f_c'}$ (MPa) was used in design. The main features of the test specimens are summarized in Table 3.1.

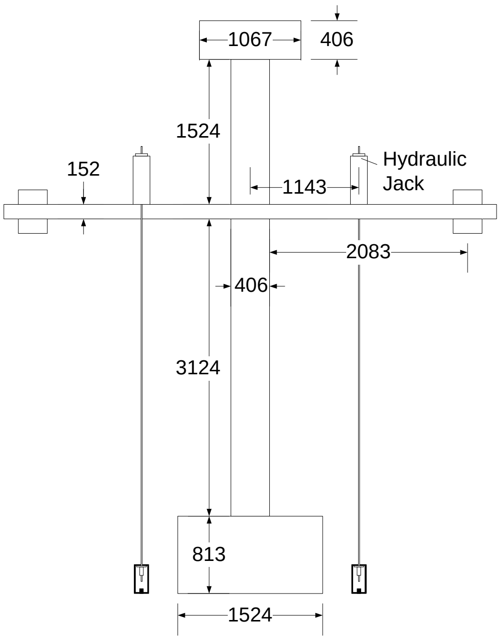

Figure 3.1. Elevation view of slab-column subassembly (dimensions in mm)

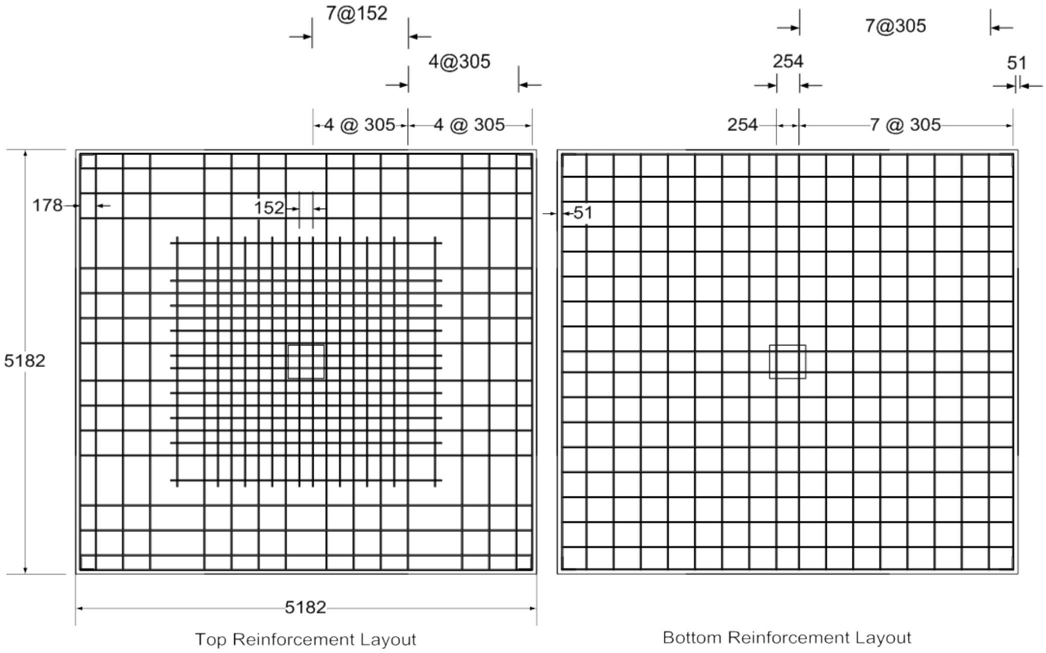

Figure 3.2. Slab flexural reinforcement (dimensions in mm)

The amount of shear reinforcement in Specimen CR-1/4 was selected such that the nominal shear capacity of the connection was greater than the shear demand imposed under the applied gravity load and the expected unbalanced moment in either of the two perpendicular directions. This led to a shear reinforcement amount governed by the minimum in Chapter 11 of the ACI Code (ACI Committee 318, 2008). The shear reinforcement in Specimens CR-0 and RA-0, on the other hand, was designed such as to resist the entire shear demand (i.e., $v_c = 0$). This led to an area of shear stud reinforcement substantially greater than the minimum specified in Chapter 21 if a shear stress check is not conducted ($v_s \geq 0.29\sqrt{f_c'}$, MPa).

Figure 3.3 shows the shear stud layout for the three specimens. All shear studs were 9.5 mm in diameter. The three shear stud layouts led to different stud spacing within each peripheral line (see Table 3.1). In terms of spacing between adjacent peripheral lines, perpendicular to the column faces, this spacing was 0.75*d* and 0.5*d* for Specimen CR-1/4 and Specimens CR-0 and RA-0, respectively. The spacing between studs on the rails oriented at 45 degrees from the column axes in Specimen RA-0, however, was set at 0.7*d* (i.e., $0.5d\sqrt{2}$) in order to facilitate placement of the slab flexural reinforcement.

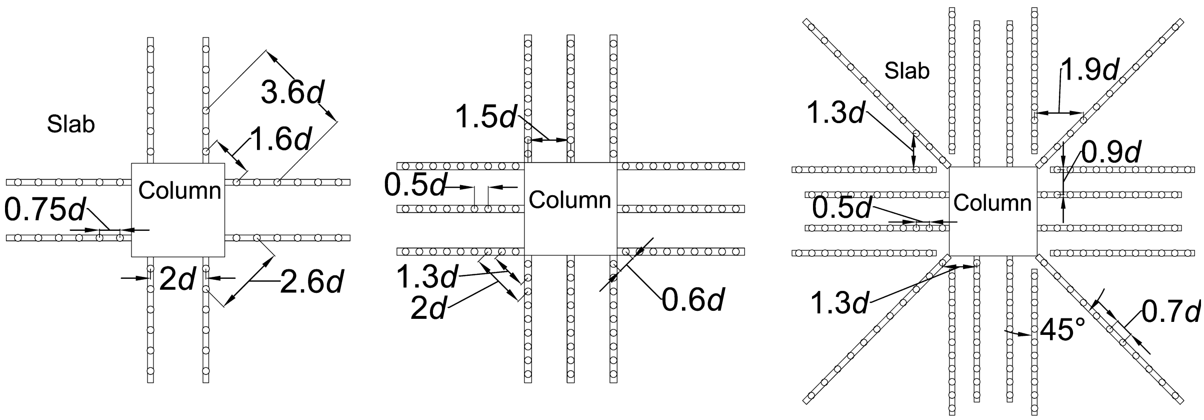

a) Specimen CR-1/4 b) Specimen CR-0 c) Specimen RA-0

d: slab effective depth = 120 mm

Figure 3.3 Slab shear stud reinforcement

Table 3.1. Main Features of Test Specimens

Specimen	f'_c, MPa	f_y (slab bars), MPa	f_y (studs), MPa	Stud spacing		v_s† ($\sqrt{f'_c}$, MPa	Peak shear stress, $\sqrt{f'_c}$, MPa††	Drift capacity‡
				Radial	Peripheral**			
CR-1/4	44.5	450	345*	0.75*d*	2*d*/2.6*d*/3.6*d*	0.18/0.16	0.36/0.48	0.90/1.25
CR-0	40.8	465	480	0.5*d*	1.5*d*/1.5*d*/2*d*	0.39/0.36	0.35/0.46	1.85/2.60
RA-0	41.9	465	345*	0.5*d*/0.7*d*	1.3*d*/1.3*d*/1.3*d*	0.53/0.48	0.36/0.50	2.30/3.25

* Nominal yield strength (actual yield strength not available)

** Maximum stud spacing within a peripheral line for first three peripheral lines

† First number based on design f'_c of 34.5MPa and second number based on cylinder strength at or near test day. Stud yield strength was limited to 420 MPa in Specimen CR-0, as specified in 2008 ACI Building Code. For Specimen RA-0, the average number of studs for the first two peripheral lines (16) was used (see Figure 3.3c)

†† From eccentric shear model applied to uni-axial and bi-axial bending and using test day concrete strength

‡ Drift for last completed cycle sustaining applied gravity load. First number is maximum drift parallel to column axes and second number is resultant drift

3.2 Simulation of Gravity Load

One of the main challenges in the testing of slab-column subassemblies is the simulation of gravity load, particularly where the target gravity shear ratio is high. In most lateral displacement tests of slab-column subassemblies with shear stud reinforcement (see for example, Megally and Ghali, 2000), gravity load has been simulated by jacking of the column at its base. While convenient, this method for simulating gravity load has significant drawbacks, including: 1) gravity and lateral load-induced shear become linked which, besides leading to an unrealistic moment-to-shear ratio, causes fictitious reductions in gravity load during cycles leading to slab flexural yielding; and 2) reductions in gravity load due to redistribution of load to the slab edge supports caused by cracking and yielding in the slab are compensated by further jacking of the column, with the associated change in the relationship between specimen drift and slab deformation demands.

In this investigation, gravity load in excess of the self-weight of the slab was simulated through the use of prestressing strands pulling down on the slab at four locations a distance of 0.94 m from each column face (see Figure 3.1). The applied gravity shear throughout the tests was obtained by monitoring the forces in the four strands, as well as the forces in the four actuators supporting the slab. This method of simulating gravity load ensured that there was always gravity load around the column, with a magnitude independent of the slab shear induced by the application of lateral displacements.

3.3 Loading Sequence and Bi-axial Lateral Displacement Demand

Prior to the application of any load to the test specimens, the four actuators supporting the slab corners were set in load control such that the force in each actuator remained at zero. A column axial load approximately equal to $0.07A_gf'_c$, where A_g is the gross area of the column, was first applied. Once the column axial load was applied, the actuators supporting the slab were set to displacement control and their current displacement locked. The prestressing strands were then tensioned until the target gravity shear was achieved, followed by the application of lateral displacements.

The lateral displacements were applied through a stiff steel crosshead attached to a block at the top of the concrete column. The 13-step cloverleaf loading pattern and the target drifts for each cycle are shown in Figure 3.4. The cloverleaf pattern is the same as that used by Pan and Moehle (1988) on slab-column connections without shear reinforcement.

After each drift cycle, the force in the strands was adjusted to maintain the desired level of gravity shear. The force in the strands was also adjusted during a drift cycle if the drop in gravity shear exceeded approximately 20%.

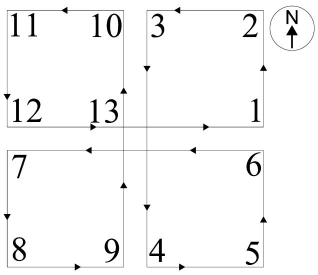

a) Clover-leaf displacement pattern per cycle

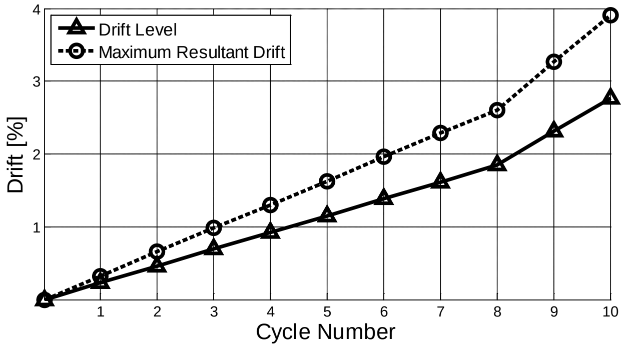

b) Drift history

Figure 3.4. Loading history

3.4 Material Properties

Cylinder compressive strength at or near the test day for the concrete used in the slabs is listed in Table 3.1, as well as yield strengths for the slab reinforcing bars and shear studs.

4. EXPERIMENTAL RESULTS

4.1 Hysteresis Behavior and Failure Mode

The lateral load versus drift response for loading in the North-South direction (parallel to one of the column axes) for the three test specimens is shown in Figure 4.1. Drift was calculated as the applied lateral displacement divided by the column height. Unless noted otherwise, reported drift values refer to each perpendicular direction.

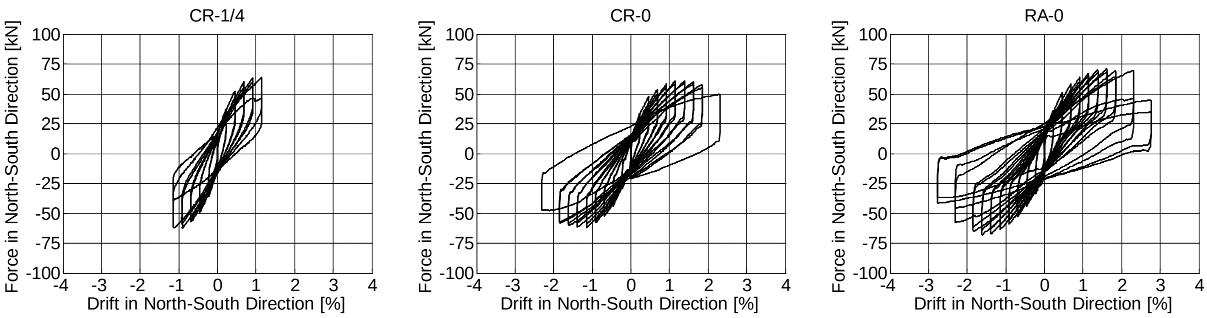

Figure 4.1. Hysteresis behavior

The behavior of the three test specimens was very similar up to the loading cycles at 0.90% drift. Flexural cracking typically started during the cycles at 0.25% and 0.45% drift, while yielding of the slab flexural reinforcement first occurred in the top middle bars near the column faces during the cycles at 0.70% and 0.90% drift. During the cycle at 1.15% drift, a punching shear failure developed in Specimen CR-1/4, leading to a drop of lateral strength and, more importantly, an inability to sustain the applied gravity load. The punching shear failure in this specimen consisted of a concrete breakout failure in the second line of studs following the formation of a diagonal crack crossing these studs. Once this breakout failure occurred, the rail supporting the studs was engaged as a dowel, leading to severe bending of the rails (Figure 4.2).

Contrary to Specimen CR-1/4, Specimens CR-0 and RA-0 exhibited no signs of distress during the cycle at 1.15% drift. The peak lateral force at this drift level was nearly the same for all three specimens, governed by flexural yielding of the slab. In Specimens CR-0 and RA-0, the peak force per cycle remained relatively constant through the cycles up to 1.85% drift, the displacement at which signs of punching-related distress in the slab-column connection became evident (Figure 4.3). Despite the punching-related damage, these two specimens were capable of sustaining the applied gravity load through the end of the cycle at 1.85% drift.

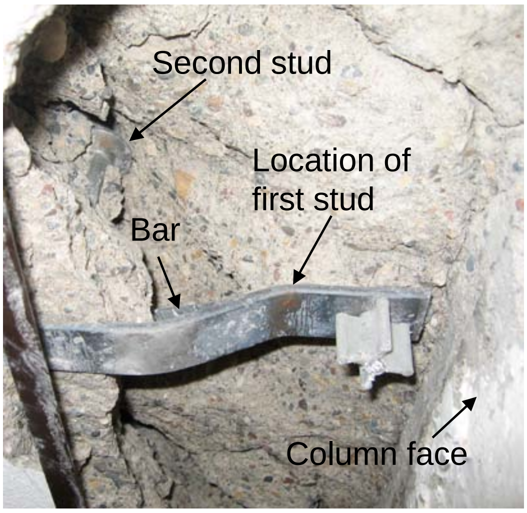

Figure 4.2. Punching failure in Specimen CR-1/4 (bottom of slab)

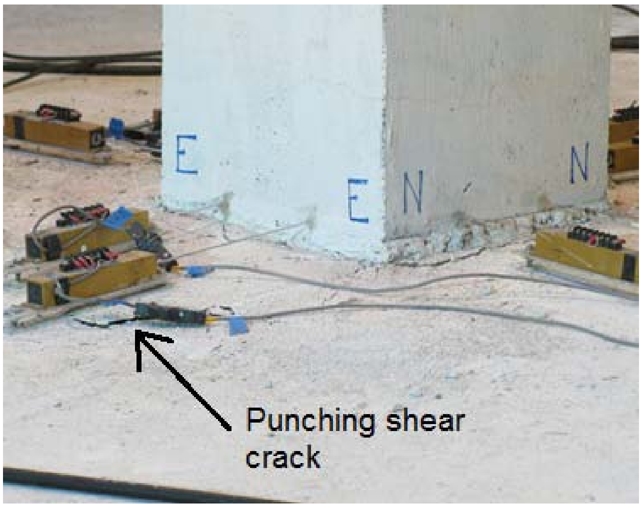

Figure 4.3. Initiation of punching shear failure during cycle at 1.85% drift in Specimen CR-0

Early during the cycle at 2.3% drift, there was a steep decline in gravity shear ratio for Specimen CR-0 as a punching shear failure developed, accompanied by a decrease in lateral strength. The force in the prestressing strands used to simulate gravity load was subsequently increased to its initial value in order to restore the desired level of gravity shear and resume the loading pattern within the 2.3% drift cycle. As the application of lateral displacement continued, however, another significant drop in the applied gravity shear occurred and further efforts to restore the gravity load were unsuccessful as the slab continued to slide down the column with little increase in gravity shear. The condition of the connection in Specimen CR-0 after completion of the test is shown in Figure 4.4. Punching shear-related damage on the North-East and North-West side of the connection consisted of diagonal cracks originating at the North column corners and propagating diagonally towards the slab regions unreinforced in shear (i.e., between perpendicular rails framing into a single column corner. On the East, South and West faces of the connection, on the other hand, damage consisted primarily of crushed and nearly pulverized concrete between the first line of studs and the column faces, as well as in between stud rails. In some cases, substantial bending of shear studs anchored by a slab top bar, accompanied by a smaller slab drop at these locations, was observed (see circled stud in Figure 4.4). This suggests that shear stud reinforcement adjacent to the column faces can be made more effective by having their top heads supported or engaged by the top slab bars passing through the column. Bending of the bottom rails was also observed, indicating some contribution to punching shear resistance through dowel action.

In Specimen RA-0, the first substantial decrease in lateral force was observed when pushing to point 6 in the loading pattern (see Figure 3.4a) during the cycle at 2.3% drift. From this point forward in the test, the hysteresis loops indicated a large decrease in specimen lateral stiffness and strength. The connection gravity shear also became very unstable beyond this point, requiring the slab to be reloaded to restore the desired level of gravity shear. By the end of the cycle at 2.3% drift, the slab had dropped a substantial amount (more than 2.5 cm), but the connection was still capable of holding the required gravity shear. Specimen RA-0 was then cycled at 2.75% drift, but the severe damage in the connection region led to the termination of the test. Failure in this specimen was characterized by substantial crushing and degradation of concrete in between the first line of studs and the column faces (Figure 4.5). Limiting stud spacing to less than 1.5*d* for the first three peripheral lines seemed to have inhibited a punching failure in which diagonal cracks propagate out of the column corners, as observed in the North-East and North-West corners of the connection of Specimen CR-0 (Figure 4.4). The use of a more uniform distribution of shear studs in Specimen RA-0 also helped delay concrete degradation in the connection, which likely led to the increased drift capacity compared to Specimen CR-0. The failure mode exhibited by Specimen RA-0 suggests that further enhancements in drift capacity would require the use of confinement reinforcement near the column faces in order to maintain the integrity of the concrete under the combined action of shear stresses and inelastic deformations.

Figure 4.4. Connection damage in Specimen CR-0 at end of test (after removal of loosed concrete)

Figure 4.5. Connection damage in Specimen RA-0 at end of test

4.2 Peak Shear Stresses

The shear stress on each face of the critical perimeter due to direct gravity shear and unbalanced moment in each principal direction were calculated using the “eccentric shear model” as specified in

Section 11.11.7 of the ACI Code (ACI Committee 318, 2008).

The peak shear stress on the critical section in each principal loading direction was nearly identical for all three specimens, with values of approximately $0.35\sqrt{f_c'}$ (MPa). The peak shear stress at corner points on the critical perimeter due to biaxial bending was also nearly identical, with values ranging from $0.46\sqrt{f_c'}$ (MPa) to $0.50\sqrt{f_c'}$ (MPa). The similarities between the shear stress demands in all three specimens are due to the fact that peak unbalanced moment was governed by flexural yielding of the slab.

Using the f'_c measured on the day of the test, the nominal shear stress capacities were $0.41\sqrt{f_c'}$, $0.61\sqrt{f_c'}$ and $0.67\sqrt{f_c'}$ (MPa) for Specimens CR-1/4, CR-0 and RA-0, respectively. For Specimen CR-0, the design yield strength of the shear studs was limited by the maximum value allowed in the ACI Code of 420 MPa. For Specimens CR-1/4 and RA-0, on the other hand, the nominal stud yield strength of 345 MPa was used due to lack of a measured yield strength. The nominal shear stress capacity of Specimen RA-0 was governed by the upper shear stress limit specified in the 2008 ACI Code.

The peak stress demand when considering unbalanced moments in each direction separately were considerably lower than the capacities predicted by the ACI Code. Further, for Specimens CR-0 and RA-0, the shear stress capacity was substantially greater than the peak shear stress calculated considering unbalanced moments in two directions acting simultaneously. It should be mentioned that the ACI Code does not recognize any reduction in the “concrete” contribution to shear strength for two-way slabs subjected to earthquake-induced displacements. The increase in drift capacity in the specimens designed with $v_c = 0$ compared to Specimen CR-1/4, however, supports such reduction.

4.3 Strains in Shear Stud Reinforcement

The axial strain in several stud shanks was monitored in Specimens CR-0 and RA-0. A relatively large increase in strain was achieved during the 0.90-1.15% drift cycles for both specimens, indicating the development of diagonal cracking in the connection region. Although strains in some of the shear studs were near the yield strain, there was no indication that yielding occurred in any of the shear studs. In general, the strains in the shear studs in Specimen CR-0 were higher than those in Specimen RA-0. This was likely due to the larger area and more even distribution of shear reinforcement provided in Specimen RA-0.

4.4 Strains in Slab Flexural Reinforcement

Strains at various locations in the top and bottom slab flexural reinforcement were monitored through strain gauges. First yielding typically occurred in the top central bars at sections adjacent to the column faces during the cycle at 0.90% drift. In Specimen CR-1/4, which failed during the cycle at 1.15% drift, peak tensile strains were approximately 0.012 in the top middle bars, with peak strains near yield measured on the bars at $b_{col}/2+h$ from the center of the connection, where b_{col} is the column width and h is the slab thickness. At this stage, similar strains were also measured in Specimens CR-0 and RA-0. By the cycle at 1.85% drift, yielding had already spread to the top slab bars within $b_{col}+2h$ for both Specimens CR-0 and RA-0. All bottom slab bars behaved in the linear elastic range prior to punching.

5. CONCLUSIONS

Results from three nearly full-scale tests of slab-column subassemblies under combined gravity load (gravity shear ratio of 0.5) and bi-axial lateral displacements were presented. All test specimens ultimately failed by punching, but drift capacity varied between 0.90% and 2.30% in each direction

(1.25% and 3.25% resultant drift) depending on the amount and distribution of shear studs. The largest drift capacity was exhibited by the specimen in which shear studs were designed to resist the entire shear demand due to gravity load and unbalanced moment (i.e., $v_c = 0$), with spacing limited to 0.5*d* between adjacent stud peripheral lines and to 1.5*d* between studs within the first three peripheral lines. The use of a more uniform distribution of shear studs seemed to have helped delay concrete degradation in the connection, which was the likely reason for the increased drift capacity. The failure mode exhibited by this specimen, however, suggests that further enhancements in drift capacity would require the use of confinement reinforcement near the column faces in order to maintain the integrity of the concrete under the combined action of gravity shear stresses and inelastic deformations.

AKCNOWLEDGEMENT

This research was sponsored by the US National Science Foundation Network for Earthquake Engineering Simulation (NEES) Program under Grant Nos. CMMI 0421180 and CMMI 0936519, the Charles Pankow Foundation, and the Concrete Research Council of the American Concrete Institute. The opinions expressed in this paper are those of the writers and do not necessarily express the views of the sponsors.

REFERENCES

ACI Committee 318. (2008). Building Code Requirements for Reinforced Concrete and Commentary (ACI 318-08), American Concrete Institute, Farmington Hills, Michigan, 465 pp.

ACI-ASCE Committee 352. (1989). Guide for Design of Slab-Column Connections in Monolithic Concrete Structures (352.1R-11), American Concrete Institute, Farmington Hills, 28 pp.

Cheng, M.-Y., Parra-Montesinos, G.J. and Shield, C.K. (2010). Shear strength and drift capacity of fiber reinforced concrete slab-column connections subjected to bi-axial displacements. *Journal of Structural Engineering* **136:9**, 1078-1088.

Comité Européen de Normalisation. (2004). Eurocode 2: Design of Concrete Structures — Part 1-1: General Rules and Rules for Buildings, English Version, EN 1992-1-1:2004: E, Brussels, Belgium, 225 pp.

Dilger, W.H. and Ghali, A. (1981). Shear reinforcement for concrete slabs. *Journal of Structural Division* **107:12**, 2403-2420.

Megally, S. and Ghali, A. (2000). Seismic behavior of slab-column connections. *Canadian Journal of Civil Engineering*. **27:1**, 84-100.

Pan, A. A. and Moehle, J. P. (1988). Reinforced Concrete Flat Plates under Lateral Loadings: An Experimental Study Including Biaxial Effects."*Report.No. UCB/EERC-88/16*, Earthquake Engineering Research Center, Univ. of California at Berkeley, Berkeley, Calif.

Widianto, Bayrak, O., and Jirsa, J. O. (2009). Two-way shear strength of slab-column connections: Reexamination of ACI 318 provisions. *ACI Structural Journal* **106:2**, 160-170.